SOUNDING OF STRATOSPHERIC OZONE WITH AN UV BIFREQUENCY DIAL: METHODS FOR SOLVING THE INVERSE PROBLEM AND RESULTS OF THE FIELD EXPERIMENT

A.V. El'nikov, V.V. Zuev, M.Yu. Kataev, V.N. Marichev, and A.A. Mitsel

Institute of Atmospheric Optics, Siberian Branch of the Russian Academy of Sciences, Tomsk
Received March 12, 1992

Three methods for inverting the lidar ozone data based on smoothing spline functions, regularization, and optimal parametrization are considered. The regularization method is shown to be inefficient for the number of gates more than 15. The possibility of employing the optimal parametrization method for processing of the lidar data is studied for the first time. The results of processing of the lidar returns from the stratosphere over Tomsk are given in this paper.

INTRODUCTION

Although the laser sounding of stratospheric ozone with an UV–bifrequency DIAL has been carrying out by a number of groups for about ten years,[1–4] the problem of reliability of lidar data inversion has not yet been solved.

The determination of the vertical profile of ozone content from lidar returns obtained with a bifrequency lidar is reduced to the problem of differentiation of the function $f(z)$:

$$f(z) = \frac{1}{2} \ln \frac{U_{of}(z)}{U_{on}(z)} + \psi(z) ; \qquad (1)$$

$$\psi(z) = \frac{1}{2} \ln \frac{\beta_{on}(z)}{\beta_{of}(z)} - (\tau_{on}(z) - \tau_{of}(z)) ,$$

where $U_{of}(z)$ and $U_{on}(z)$ are the lidar returns at the distance z at the wavelengths λ_{of} and λ_{on}, $\beta_{of}(z)$ and $\beta_{on}(z)$ are the backscattering coefficients at the wavelengths λ_{of} and λ_{on}, and $\tau_{on}(z)$ and $\tau_{of}(z)$ are the optical thicknesses of molecular scattering and aerosol extinction.

It is assumed in Eq. (1) that $U_{of}(z)$ and $U_{on}(z)$ are free of the signals of the atmospheric background radiation. The function $\psi(z)$ is assigned starting from model representations or is determined from an independent experiment.

The ozone concentration is defined as

$$\rho(z) = \frac{1}{2\Delta K(z)} \Phi(z) , \qquad (2)$$

where $\Phi(z)$ is the regularized analog of the derivative $f'(z)$ of the function $f(z)$ and ΔK is the differential cross section of the O_3 absorption.

It is well known[5] that the problem of differentiating the experimental information is classified among the ill–posed problems. This is manifested in the solution stability violation,[6] i.e., insignificant errors in the initial data can lead to large errors in the solution (the solution gets loose) and, in some cases, to the occurance of negative magnitudes of gas concentration.

At present, a number of methods[7–17] are used for solving problem (10). In this paper we try to compare the three methods of inverting the function $f(z)$: the method of spline function,[7–8] the method of the Tikhonov's regularization,[11–16] and the method of optimal parametrization. The third method has not yet been used for processing of the lidar ozone data, therefore the efficiency and conditions for applying this method are studied in our paper.

1. THE METOD OF SPLINE FUNCTION

This method is based on preliminary smoothing of the function $f(z)$ and subsequent differentiation of the smoothed function. The method was first applied to processing of the data of lidar sounding of the H_2O vapor.[7–8] A cubic spline was used for smoothing.[18] The method to construct a smoothing spline was considered in detail in monographs (see, e.g., Ref. 19), therefore we shall give only a brief description of the basic relations.

Let the function $f(z)$ be preset by its measured values $f(z_i) = f_i$ at the nodes of the grid z_i:
$a = z_1 < z_2 < \ldots < z_{n-1} < z_n = b$. A smoothing cubic spline $S_{n\alpha}$ is the solution of the variational problem

$$F_\alpha = \inf \left\{ \alpha \int_a^b [S''(z)]^2 dz + \sum_{i=1}^{n} p_i [f_i - S_i]^2 \right\} ; \qquad (3)$$

$S(z) \in C^2[a, b]$

and is represented on each segment $h_i = z_{i+1} - z_i$ by the third–degree polynomial

$$S_{n\alpha} = a_i + b_i(z - z_i) + c_i(z - z_i)^2 + d_i(z - z_i)^3 \qquad (4)$$

with the continuous derivatives $S'_{n\alpha}(z)$ and $S''_{n\alpha}(z)$.

The spline coefficients a, b, c, and d are expressed in terms of the elements of the vector of the second–order derivatives $M_{i+1} = \{m\}_i$ which are the solution of the system of linear equations

0235-6880/92/06 362-08 $02.00

$$(\alpha HP^{-1}H^{\mathrm{T}} + A)m = Hf \qquad (5)$$

with the boundary conditions $M_1 = M_n = 0$.

Here α is the scalar ($\alpha > 0$) which has the meaning of the smoothing parameter. The components of the matrices H and A are expressed in terms of the elements of the sequence $h_i = z_{i+1} - z_i$:

$$A_{i,i} = (h_i + h_{i+1})/3\ ,\ i = 1,\ \ldots,\ n-2\ ;$$

$$A_{i,i+1} = A_{i+1,i} = h_{i+1}/6\ ,\ i = 1,\ \ldots,\ n-3\ ;$$

$$H_{i,i} = 1/h_i\ ;\ H_{i,i+1} = -(1/h_i + 1/h_{i+1})\ ,\ i = 1,\ \ldots,\ n-2\ ;$$

$$H_{i,i+2} = 1/h_{i+1}\ ,\ i = 1,\ \ldots,\ n-2\ ;$$

where P is the diagonal matrix: $P = \mathrm{diag}\{p_1,\ \ldots,\ p_n\}$.

System (5) with the symmetric positively determined five–diagonal $(n-2)*(n-2)$ matrix has a unique solution and is calculated by the pass technique.[18] After finding the elements of the vector $\{m\}_i = M_{i+1}$, $i = 1,\ \ldots,\ n-2$, the spline coefficients $S_{n\alpha}(z)$ are determined from the relations[19]

$$a_i = f_i - \{\alpha F^{-1}H^{\mathrm{T}}m\}_i\ ,\quad i = 1,\ \ldots,\ n\ ;$$

$$b_i = (a_{i+1} - a_i)/h_i - h_i(2M_i + M_{i+1})/6\ ,\quad i = 1,\ \ldots,\ n-1\ ;$$

$$c_i = M_i/2\ ,\quad d_i = (M_{i+1} - M_i)/6h_i\ ,\ i = 1,\ \ldots,\ n-1\ .$$

The accuracy of construction of the spline $S_{n\alpha}(z)$ depends strongly on the value of the smoothing parameter. At present, there are different criteria for searching α (see Ref. 19). We use here three criteria: optimal, statistical principle of discrepancy, and a criterion of discrepancy. All of these criteria preassume the knowledge of the error in the measurement of the function $f(z)$. At the same time, the first two criteria require the information about the measurement error at each node z, while the third criterion requires that the averaged error for the entire range $[z_1,\ z_n]$ be known. There also exists a criterion for selecting α in the case of the unknown matrix of the measurement noise.[8,19]

The method of spline functions as applied to the solution of problem (1) was further developed in Ref. 10, where the procedure for constructing the descriptive cubic splines was suggested. The advantage of this approach is the possible application of an *a priori* information about $f'(z)$ in the form of inequalities (e.g., $f''(z)) > 0$).

2. THE REGULARIZATION METHOD

The Tikhonov regularization method for processing the lidar data was first used in Ref. 11 for solving the problem of sounding of the tropospheric humidity. In their subsequent papers[12–15] the authors suggested that the lidar returns be processed separately for each wavelength. As applied to the solution of problem (1), the technique of calculation of the derivative $\Phi(z) = f'(z)$ has the form[14,15]

$$\Phi(z) = \frac{1}{2}\left[(\ln U_{\mathrm{of}}(z))' - (\ln U_{\mathrm{on}}(z))'\right] + \psi'(z)\ , \qquad (6)$$

where the regularized analogs obtained from the solution of the Fredholm equation of the first kind are used as $(\ln U_{\mathrm{of}}(z))'$ and $(\ln U_{\mathrm{on}}(z))'$. This approach, in spite of the twofold increase of computation time, turns out to be useful in processing of the integrated lidar returns at the wavelengths λ_{of} and λ_{on} individually. In our problem we propose simultaneous integration of signals at two wavelengths; therefore, $f(z)$ related to the measured lidar returns via relation (1) is used as a processable function.

The regularized solution $\Phi(z) = f'(z)$ for problem (1) is determined from the Fredholm equation of the first kind

$$\int_a^b K(x,\ z)\ \Phi(z)\ \mathrm{d}z = g(x)\ ; \qquad (7)$$

$$g(x) = \int_x^b f(y)\ \mathrm{d}y - f(a)(b - x)\ ; \qquad (8)$$

$$K(x,\ z) = \begin{cases} b - x\ ,\ x \ge z \\ b - z\ ,\ x < z\ . \end{cases} \qquad (9)$$

The transformation to algebraic form (7) is accomplished for the uniformly spaced grid with the step $h = z_{i+1} - z_i$. The formula of rectangles on a grid displaced at $h/2$ is used as a numerical quadrature. The algebraic analog in a matrix form is

$$K\Phi = g\ , \qquad (10)$$

where k is the $(n-1)*(n-1)$ matrix with the elements

$$K(x,\ z) = \begin{cases} b - a - h(i - 0.5),\ i \ge j \\ b - a - h(j - 0.5),\ i < j\ , \end{cases}$$

Φ is the $(n-1)$ – dimensional vector of the derivative $f'(z)$ which is assigned at the nodes of the grid $z_i + h/2$, g is the $(n-1)$ – dimensional vector of the right side determined at the nodes of the displaced grid.

The regularized solution of problem (10) with the use of a first–order stabilizer is written down in the form[6]

$$\Phi_\alpha = (K^{\mathrm{T}}K + \alpha B)^{-1}K^{\mathrm{T}}g\ , \qquad (11)$$

where β is the finite–dimensional analog of the stabilizer derivative which has the form of a tridiagonal $(n-1)*(n-1)$ matrix with the elements

$$B_{11} = p_1 + q_1/h^2\ ;\ \ B_{n-1,n-1} = p_{n-1} + q_{n-1}/h^2\ ;$$

$$B_{ii} = p_i + (q_{i+1} + q_i)/h^2\ ,\ i = 2,\ \ldots,\ n-2\ ;$$

$$B_{i,i+1} = B_{i+1,i} = -q_i/h^2\ ,\ i = 1,\ \ldots,\ n-1\ ;$$

where p_i and q_i are the weighting functions $p(z)$ and $q(z)$ at the nodes of the grid z_i.

The unknown parameter α (the regularization parameter) enters into Eq. (1). In our paper the parameter α is chosen against one of the two criteria: discrepancy or statistical discrepancy.

3. METHOD OF OPTIMAL PARAMETRIZATION

This method is widely used for solving the problems of spaceborne sounding of the atmosphere (see, e.g., Ref. 21). Let us consider its possible applications to the problem of lidar sounding of ozone.

The unknown function $\Phi(z) = f'(z)$ is represented in the form

$$\Phi(z) = \bar{\Phi}(z) + \tilde{\Phi}(z) , \qquad (12)$$

where $\bar{\Phi}(z)$ is the mean value of the function derived from the data of long standing and $\tilde{\Phi}(z)$ is the deviation from the mean value.

Upon substituting Eq. (12) into Eq. (7), we obtain

$$\int_a^b K(x, z)\, \tilde{\Phi}(z)\, dz = \tilde{g}(x) ; \qquad (13)$$

$$\tilde{g}(x) = g(x) - \int_a^b K(x, z)\, \Phi(z)\, dz . \qquad (14)$$

The unknown function here is $\tilde{\Phi}(z)$. The regularized solution of Eq. (11) with the right side $\tilde{g}(x)$ can be used as $\tilde{\Phi}(z)$. Such an approach was employed in Ref. 16, in which the profile $K_{O_3}(z) \cdot \bar{\rho}(z)$ of the Krueger model was taken as $\bar{\Phi}(z)$. Here K_{O_3} is the ozone absorptional cross section and $\bar{\rho}(z)$ is the average profile of ozone.

However, the solution of $\tilde{\Phi}(z)$ can be found differently. Let us assume that in addition to the mean value $\bar{\Phi}(z) = K_{O_3}(z)\bar{\rho}(z)$, the empirical eigenvectors of ozone $t_k(z)$, $k = 1, \ldots, m$ are also known. We now expand $\Phi(z)$ into a series in the system $t_k(z)$

$$\tilde{F}(z) = K_{O_3}(z) \sum_{k=1}^{m} b_k t_k(z) . \qquad (15)$$

The optimal parametrization means that this system with the preset number of eigenvectors $t_k(z)$, provides minimum variance of the residual term of the expansion compared to any other orthonormalized system of functions.[20] In practice, the first eigenvectors corresponding to the maximum eigenvalues are used as a rule. Thus, for the humidity profile it is sufficient to use two or three first eigenvectors, and the residual variance will be < 10% (see Ref. 10). For ozone, it is necessary to substitute into Eq. (15) from six to eight vectors to provide the variance of the residual term ≈ (5–8)% (see Refs. 22 and 23), i.e., of m vectors it is sufficient to take $\tilde{m}$ = 6–8 vectors $t_k(z)$.

By substituting Eq. (15) into Eq. (13), we obtain the system of linear equations for the unknown coefficients b_k

$$\sum_{k=1}^{\tilde{m}} R_{ik} b_k = \tilde{g}_i , \qquad (16)$$

where

$$R_{ik} = \sum_{j=1}^{n-1} K_{ij} t_k(j) , \quad k = 1, \ldots, \tilde{m} .$$

Solution (16) obtained by the least–squares technique is given in the form

$$b = (R^T R)^{-1} R^T \tilde{g} . \qquad (17)$$

Here we have the system of linear equations in m unknowns. Having calculated the coefficients b_k from Eq. (17) we can reconstruct $\Phi(z)$ using formulas (15) and (12).

It should be noted that the method for optimal parametrization does not provide the stable solution of the inverse problem. Therefore, in addition to Eq. (17), we also consider the regularized solution

$$b^{\alpha} = (R^T R + \alpha I)^{-1} R^T \tilde{g} \qquad (18)$$

with insignificant distortion of the matrix of the system ($\alpha = 10^{-6}$) which makes it possible to obtain a stable solution in all numerical experiments given that the noise level $\delta \le 0.1$.

4. NUMERICAL EXPERIMENT

A comparison between the spline–function and regularization methods was made at the first stage of numerical simulation. For the numerical simulation the following function was chosen

$$\Phi(x) = \exp\{- \ln(2)\, ((x - 0.5)/0.25)^2\}$$

using it we calculated the function $f(z) = \int_0^z \Phi(x)\, dx$. To imitate the measurement noise, the values of the function $f(x)$ at the nodes z_i, $i = 1, \ldots, n$ were distorted with the use of the generator of normally random variables whose variance was equal to $\sigma_i^2 = \delta^2 \cdot f_i^2$, where δ is the relative error (the measurement noise).

Let us now analyze the results of numerical experiments on comparison of the solutions Φ_{sp} and Φ_{reg} obtained using a cubic smoothing spline (sp) and the Tikhonov regularization method (reg). The smoothing and regularization parameters in both methods were determined against the criterion of statistical discrepancy. The number of nodes n increased from 10 to 40 .

Depicted in Fig. 1 are the results of reconstructing Φ_{sp} (curve *2*) and Φ_{reg} (curve *3*) for different number of nodes and the noise levels δ = 0 and 1%. The rigorous solution Φ (curve *1*) is also presented here for comparison. As the number of nodes n increases, the error in the reconstruction of Φ_{reg} increases faster than the error in the reconstruction of Φ_{sp} does. Thus, when the number of nodes n = 30 even for the zeroth noise level we observed ripples in the solution Φ_{reg} (Fig. 1*c*), and when n = 40 the solution Φ_{reg} got loose (Fig. 1*d*).

The efforts to improve the solution Φ_{reg} by varying α did not provide the desired result. One of the approach to improve the solution Φ_{reg} is probably the refinement of the algorithm or the use of a computer with a longer word length (we used PC/AT–286). The other method to improve the solution Φ_{reg} is to change the weighting functions $p(x)$ and $g(x)$ in the matrix B (see Eq. (11)). In our numerical experiment these function were set equal to unity. In practice, it is most expedient to reconstruct Φ_{reg} on a more widely spaced grid with the number of nodes, at which the solution is found, not more than 15. As can be seen from Fig. 1 as well as from the results of simulation for different noise levels, the solution Φ_{sp} is found stably for any number of nodes and any noise level up to 5%.

By means of numerical simulation we study the effect of the noise model on the solution stability. In addition to a "normal" noise we simulated the perturabation of the $f(z)$ function by a periodic noise (an alternating one). Figure 1*h* shows one of instances of reconstructing Φ_{sp} and Φ_{reg} for $n = 30$ and for alternating noise at the level of 10%. It can be seen that Φ_{sp} is stable while Φ_{reg} starts to get loose at the last three points. It should be noted that a periodic noise is filtered much better than a conventionally normal noise. Due to this fact it becomes possible to obtain stable solutions Φ_{sp} and Φ_{reg} even for a noise level of 30%.

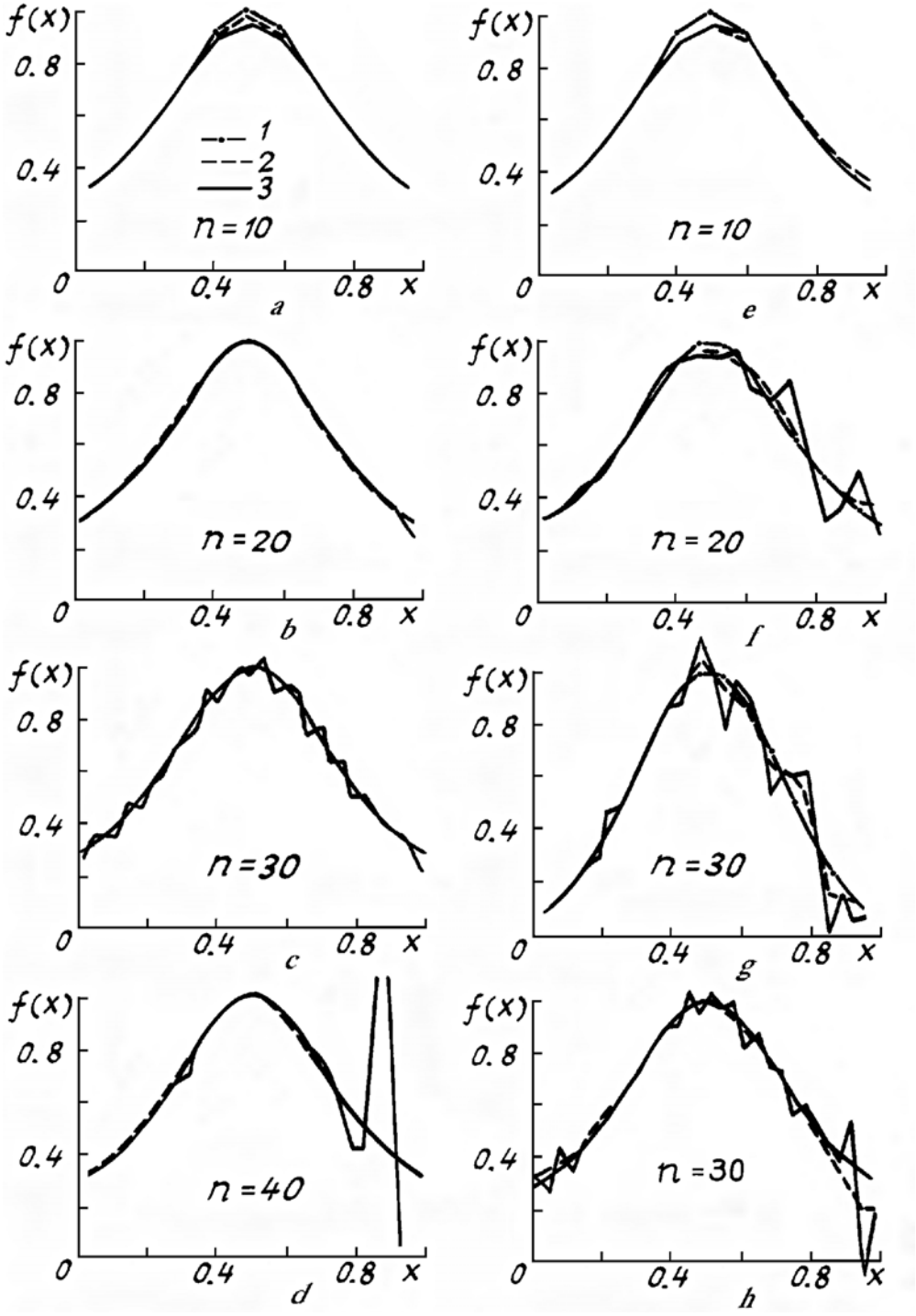

FIG. 1. Comparison of the model function reconstruction using the spline–function and regularization methods. 1) exact function, 2) reconstruction by the spline–function method, 3) reconstruction by the regularization method, a – d) 0% error; e – g) 1% error; and h) 10% error.

Let us now proceed to a numerical simulation of the efficiency of the optimal parametrization method. To do this, let us make use of the statistical information about the average content of ozone $P_{O_3}(z)$ and the covariation matrix $C_{O_3}(z, z')$ derived at the Institute of Atmospheric Optics[23] from the radiozonde data obtained at the station Gus–Bei. Based on the initial matrix C_{O_3} we constructed the eigenvectors $t_k(z)$ and calculated the eigenvalues μ_k, for $k = 1, \ldots, 27$.

The inverse problem was simulated according to the following scheme:

1) The coefficients b_k for $k = 1, \ldots, 27$ were simulated with the help of the generator of random variables with the parameters $(0, \mu_k)$.

2) A random component of the ozone pressure profile $\tilde{P}_{O_3}(z)$ was calculated from Eq. (15) and then a random ozone profile $P_{O_3}(z) = \tilde{P}_{O_3}(z)) + \overline{P}_{O_3}(z)$ was calculated.

4) The optical depth $f(z) = \int_0^z \Phi(y)\, dy$ was calculated.

5) The values of $f(z)$ so obtained at the nodes z were distorted with the help of a random generator of variables for simulating the measurement noise. Thus at this stage of simulation the function

$$\tilde{f}(z) = f(z) + \xi(z)$$

was taken as a measured function, where ξ stands for a random component.

6) The function

$$\tilde{g}(z) = g(x) - \int_a^b K(x, z)\, \overline{F}(z)\, dz ,$$

was formed, where $\tilde{\Phi}(z) = K_{O_3} \cdot \overline{P}_{O_3}(z)$. The grid over the variables x and z was taken uniformely spaced with a step of 0.5 km.

7) Inverse problem (18) was solved for b_k^a and the profile

$$\Phi_{op}(x) = \overline{\Phi}(z) + K_{O_3}(z) \sum_{k=1}^{8} b_k^a t_k(z)$$

was reconstructed.

In practice no statistical information about vertical correlations of ozone is available for a geographic site of lidar location. Therefore it is of great importance to study the efficiency of the optimal parametrization method not only with "its own" but with a "foreign" system of eigenvectors. The statistical ozone model at midlatitude was taken as a "foreign" system of eigenvectors for the Gus–Bei station.[25]

Figures 2*a* and 2*b* depict the results of reconstruction of $\Phi_{sp}(z)$ for "its own" (curve *2*) and "foreign" (curve *3*) systems of eigenvectors for two experimental schemes. In Fig. 2*a* the function $f(z)$ was considered to be known for the entire range of altitudes from 0 to 30 km ($a = 0$). In Fig. 2*b* the minimum altitude was $a = 9$ km, i.e., $f(z)$ was "measured" between 9 and 30 km.

The suggested scheme of the numerical experiment with different minimum altitudes a enabled us to analyze the possibility of reconstructing the ozone content profile in the troposphere from the data of sounding of stratospheric ozone. It can be seen from Figs. 2*a* and *b* that it is possible to determine the ozone profile for the entire range of altitudes from 0 to 30 km from the data on $f(z)$, while the information about $f(z)$ above 9.5 km (in the numerical experiment in addition to $a = 9$ km, the minimum altitudes $a = 9.5$ and 10 km were also considered) does not allow the ozone profile in the troposphere to be reconstructed with sufficient accuracy. This is due to the fact that in the 9–10–km layer (Gus–Bei station) there exists an ozone pause. In the ozone–pause layer the sign of correlation changes. For the other regions the ozone–pause altitude can differ.

The third stage of simulating the problem of lidar sounding of ozone was accomplished based on the simulated lidar returns according to the following scheme:

1) Typical parameters of the lidar system operating on the basis of the induced Raman scattering conversion of the radiation with a wavelength of 308 nm into the radiation with a wavelength of 353 nm were prescribed as follows: $\lambda_{on} = 308$ nm, $E_0^{on} = 56$ mJ, $A = 0.785$ m^2, $\Delta H = 0.4$ km (strobe length), $q_{on} = q_{of} = 8.575 \cdot 10^{-4}$ (lidar efficiency including a receiving–transmitting optical train, quantum yield of the photomultiplier, efficiency of the receiving aperture, transmission of the filter, and other losses), $\lambda_{of} = 353$ nm, and $E_0^{of} = 20$ mJ. The model coefficients of molecular scattering, aerosol extinction, and backscattering were borrowed from Ref. 25. The ozone absorption coefficients $K_{O_3} = 1.19 \cdot 10^{-19}$ cm^2 at $\lambda_{on} = 308$ nm (see Ref. 24).

2) The random ozone profile and the optical depth of ozone at λ_{on} and λ_{of} (see items 1–4 of the second stage of simulation) were simulated from the data obtained at the station Gus–Bei.

3) The lidar returns U_{on} and U_{of} were calculated with an altitude step of 0.4 km for a single pulse within the 0–30 km altitude range with the use of the lidar equation in the single–scattering approximation.

4) The obtained signals were distorted with the help of the generator of random variables with the parameters $(0, U_{on}/n)$ and $(0, U_{of}/n)$, where n is the number of pulses.

5) The function $f(z)$ was calculated using Eq. (1) starting from an altitude of 9 km. It was then used as a "measured" function.

6) The inverse problem was solved using the three above–described methods and the solutions Φ_{sp}, Φ_{reg}, and Φ_{op} were found. The solution Φ_{op} was obtained using both "its own" and "foreign" systems of eigenvectors corresponding to the averaged zonal model for the midlatitudes.[21]

Depicted in Figs. 2*c* and *d* is the intercomparison of the solutions Φ_{sp}, Φ_{reg}, and Φ_{op}. Figures 2*c* and *d* shows the solution Φ_{sp} (curve *2*) and Φ_{reg} (curve *3*) for 100 and 10 000 pulses at $a = 9$ km as well as an exact profile of the ozone absorption oefficient (curve *1*). The solution Φ_{reg} was obtained with spatial resolution $\Delta H = 1.2$ km at 14 points though the function $f(z)$ was known with spatial resolution $\Delta H = 0.4$ km at 42 points in the 9–30 km altitude range. As was shown above, for the large number of nodes the loss of stability in reconstructing the unknown function by the regularization method occurs. As can be seen from the figures, for the stable reconstruction of the ozone profile the signals must be integrated over a longer period of time.

Figures 2*e* and *f* show the intercomparison of the solutions Φ_{op} for "its own" (curve *2*) and "foreign" (curve *3*) systems of eigenvalues for a single pulse (Fig. 2*e*) and 1000

pulses (Fig. 2*f*) at $a = 9$ km compared with the exact profile (curve *1*). As can be seen from the figures, the signal integration significantly improves the quality of ozone profile reconstruction for both "its own" and "foreign" systems of eigenvectors. To reconstruct these profiles when solving the system of equations, the parameter α was taken to be 10^{-6} (see Eq. (18)).

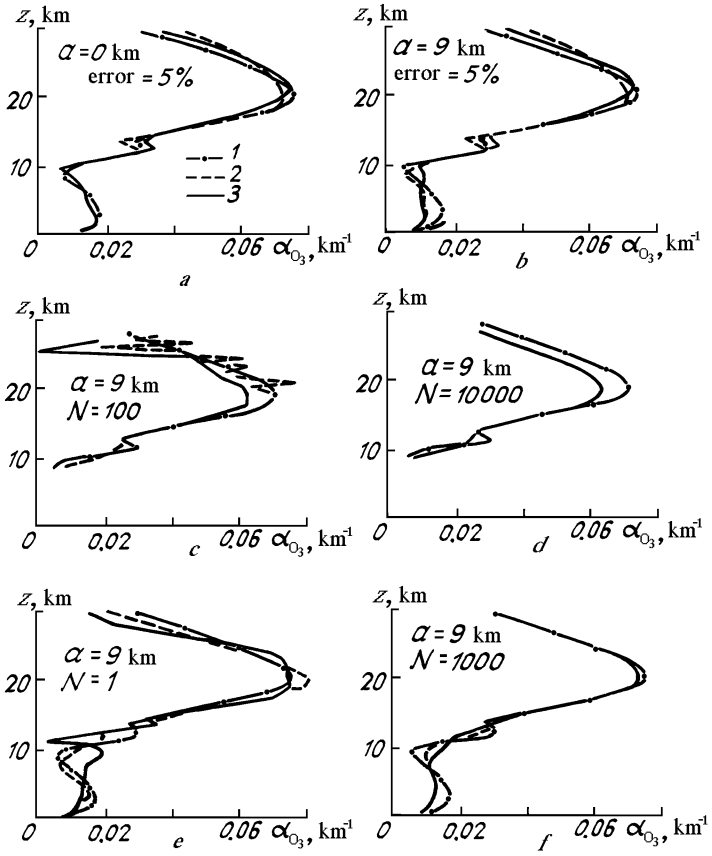

FIG. 2. Results of the solution of the inverse problem by different methods: a and b) reconstruction of the profile α_{O_3} by the optimal parametrization method based on "its own" (curve 2) and "foreign" (curve 3) systems of eigenvectors. The optical depth is taken as a "measured" function. Curve 1 is for the rigorous solution. c – f) reconstruction of α_{O_3} based on model lidar returns: c and d) the spline–function (curve 2) and regularization (curve 3) methods; e and f) the optimal parametrization method.

5. THE RESULTS OF PROCESSING THE LIDAR DATA

The lidar data on sounding of the stratospheric ozone over Tomsk were obtained in summer as part of the SATOR program on July 6, 8, 9, 11, 14, 20, 22, and 24, 1991. At some nights we obtained several runs of ozone sounding.

The laser sounding of the stratospheric ozone was carried out using a lidar with a 1–m receiving mirror and a Xe–Cl laser equipped with the converter of laser radiation intensity based on the effect of the induced Raman scattering on H_2. Blockdiagram of the lidar (Fig. 3) has the following basic parameters: the laser pulsewidth was 10 ns and the laser pulse repetition frequency was 70 Hz at $\lambda_{on} = 308$ nm and $\lambda_{of} = 353$ nm and the laser pulse energy was 60 and 8 mJ, respectively. The signals were recorded in the photocurrent pulse counting regime with gating for the gate length of $\simeq 2.5$ μs ($\Delta z \simeq 375$ m). The time of lidar signal integration over single sounding cycle was 30 min.

To process the real data, we employed the spline–function method. This method was chosen due to its highest stability with respect to the errors in the input data for any number of nodes. As was shown above, the regularization method is instable for the large number of nodes and inefficient because if requires much computational time. The decrease of the number of nodes improves the solution stability but, in this case, spatial resolution deteriorates. At present it is impossible to use the optimal parametrization method for processing of the real data due to the lack of the statistical data on the average ozone content over Tomsk. The use of the "foreign" average profile can lead to uncontrolled errors in reconstructing the ozone profile from the lidar data.

Figure 4*a* depicts the vertical ozone profiles reconstructed from the lidar returns obtained in July using cubic splines in the 15–25 km altitude range. Maximum of the ozone layer is seen to be located within the 19–21 km altitude range and this is in agreement with physical concept of the ozone layer at midlatitudes.[26]

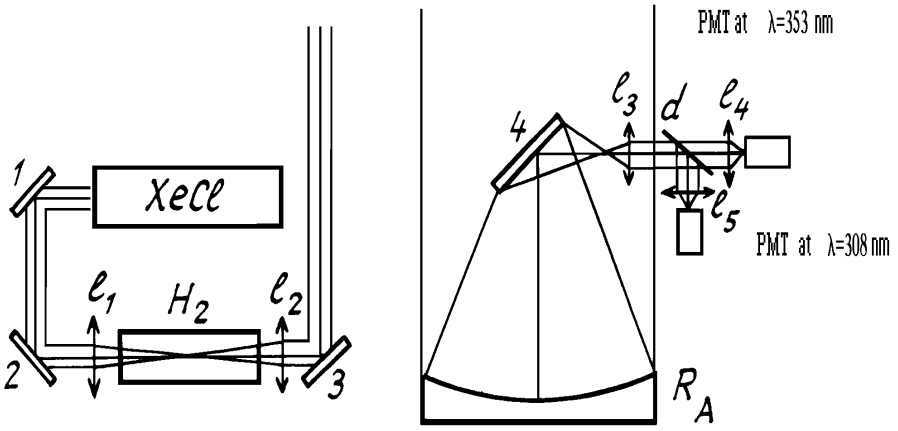

FIG. 3. Block diagram of an ozone bifrequency lidar: 1, 2, 3, and 4) rotating mirrors; ,l_1,...,l_5 denote focusing and collimating lenses; d denotes dichroic mirror, R_a denotes a receiving mirror 1 m *in diameter;* XeCl *denotes an excimer laser,* H_2 *denotes a high–pressure (*16 atm*) hydrogen cell with induced Raman scattering.*

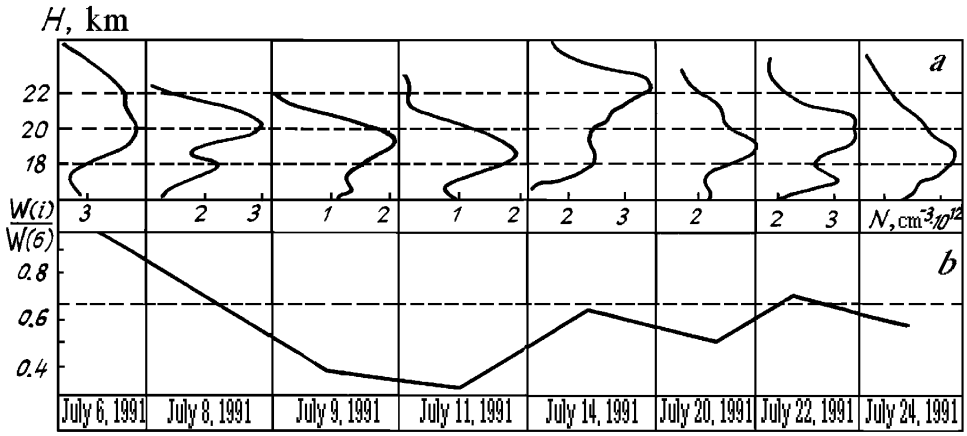

FIG. 4. Ozone profiles reconstructed from lidar returns obtained at different time (a) and relative variation of the total ozone content in the 16–23 km *altitude range (b).*

It should be noted that the variations of the ozone content in stratospheric maximum over the period of observations were very significant. Thus, e.g., an integral ozone content in the 16–23 km altitude range decreased by more than a factor of two from July 6 to July 9 (see Fig. 4*b*). At the same time, the dynamic variations were observed even at one night. Figure 5 shows four ozone profiles measured during less than two hours at night on July 11. A dashed line in this figure shows the standard deviation of the recorded profiles from the average one over the entire night period of observations.

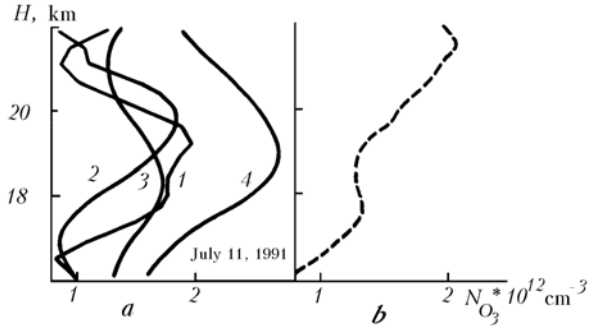

FIG. 5. Ozone profiles obtained during four runs at one night (a) and standard deviation about the average profile (b).

In accordance with the analysis of stratospheric weather maps over the indicated period of lidar observations, the air masses of subtropic origin were injected into the midlatitudes (this synoptic situation is described in the present issue). As is well known, at these altitudes in tropics there is an ozone pause with a depleted content of ozone. Thus, the results of the lidar observations of transformation of ozone profiles obtained in July are in a good agreement with synoptic data as well as with the data on ozone "depression" caused by the Pinatubo volcano eruption. Strong variations in ozone profiles at one night are most likely caused by dinamic variations of horizontal displacements of air.

In conclusion, the authors would like to thank S.A. Mikhailov for his kindly given data on the ozone covariation matrix obtained at the Gus–Bei station.

REFERENCES

1. J. Werner, K.W. Rothe, and H. Walther, Appl. Phys. **B32**, No. 3, 113 (1983).
2. H. Claude and K. Wege, in: *Abstracts of Reports at the 14th International Laser Radar Conference*, San Candido (1988), p. 392.
3. S. McDermid, S.M. Godin, et al., in: *Abstracts of Reports at the 15th International Laser Radar Conference*, Tomsk (1990), Vol. 1, p. 129.

4. H. Nakane, J. Sasano, et al., in: *Abstracts of Reports at the 15th International Laser Radar Conference*, Tomsk (1990), Vol. 1, p. 116.
5. V.B. Demidovich, *Vychislit. Metody Program.*, No. 8, 96–102 (1967).
6. A.N. Tikhonov and V.Ya. Arsenin, *Methods for Solving the Ill–Posed Problems* (Nauka, Moscow,1979), p. 238.
7. V.N. Marichev and A.A. Mitsel', in: *Abstracts of Reports at the Fifth All–Union Symposium on Laser Radiation Propagation in the Atmosphere*, Tomsk (1979), Vol. 3, pp. 192–196.
8. Yu.E. Voskoboinikov and A.A. Mitsel', Izv. Akad. Nauk SSSR, Ser. FAO **17**, No. 2, 832 (1981).
9. V.E. Zuev, V.V. Zuev, Yu.S. Makushkin, et al., Appl. Opt. **22**, No. 23, 3733–3741 (1983).
10. Yu.E. Voskoboinikov, M.Yu. Kataev, and A.A. Mitsel', Atm. Opt. **4**, No. 2, 151–158 (1991).
11. B.P.Ivanenko and V.N.Marichev, in: *Abstracts of Reports at the Fifth All–Union Symposium on Laser and Acoustic Sounding of the Atmosphere*, Tomsk (1978), pp. 61–65.
12. B.P. Ivanenko and I.E. Naats, Opt. Lett. **6**, No. 7, 305–307 (1981).
13. B.P. Ivanenko and N.D. Smirnov, in: *Abstracts of Reports at the Fifth All–Union Symposium on Laser and Acoustic Sounding of the Atmosphere*, Tomsk (1982), Vol. 2, pp. 82–85.
14. V.E. Zuev, B.P. Ivanenko, and I.E. Naats, Issled. Zemli iz Kosmosa, No. 5, 117 (1985).
15. V.E. Zuev and I.E. Naats, *Inverse Problems of Lidar Sounding of the Atmosphere* (Nauka, Novosibirsk, 1982).
16. B.P. Ivanenko, Opt. Atm. **1**, No. 8, 111–115 (1988).
17. N.S. Ivanova and G.M. Kruchenitskii, in: *Abstracts of Reports at the Eleventh All–Union Symposium on Laser Radiation Propagation in the Atmosphere*, Tomsk (1991), p. 182.
18. S.B. Stechkin and Yu.N. Subbotin, *Splines in Computational Mathematics* (Nauka, Moscow, 1976), p. 248.
19. Yu.E. Voskoboinikov, N.G. Preobrazhenskii, and A.I. Sedel'nikov, *Mathematical Processing of the Experiment in Molecular Gas Dynamics* (Nauka, Novosibirsk, 1984), p. 237.
20. A.M. Obukhov, Izv. Akad. Nauk SSSR, Geofizika, No. 3, 345 (1960).
21. M.S. Malkevich, *Optical Investigations of the Atmosphere from Satellites* (Nauka, Moscow, 1973), p. 303.
22. V.E. Zuev and V.S. Komarov, *Statistical Models of Temperature and Gas Components of the Atmosphere* (Gidrometeoizdat, Moscow, 1986), 262 pp.
23. V.S. Komarov, S.A. Mikhailov, and D.N. Romashov, *Statistical Structure of Vertical Distribution of Atmospheric Ozone* (Nauka, Novosibirsk, 1988), 76 pp.
24. R.N. Surkin, V.G. Serzhantov, and V.A. Torgovchev, in: *Atmospheric Ozone* (Gidrometeoizdat, Moscow, 1990), pp. 12–17.
25. I.I. Ippolitov, V.S. Komarov, and A.A. Mitsel', in: *Spectroscopic Methods of Sounding of the Atmosphere* (Nauka, Novosibirsk, 1985), pp. 4–44.
26. A.J. Krueger and R.A. Minzner, J. Geoph. Res. **81**, No. 24, 4477 (1976).